PROGRESS IN PHOTOVOLTAICS: RESEARCH AND APPLICATIONS
Prog. Photovolt: Res. Appl. (2012)
Published online in Wiley Online Library (wileyonlinelibrary.com). DOI: 10.1002/pip.2215

RESEARCH ARTICLE

Impact of phosphorus gettering parameters and initial iron level on silicon solar cell properties

Ville Vähänissi*, Antti Haarahiltunen, Heli Talvitie, Marko Yli-Koski and Hele Savin

Department of Micro and Nanosciences, Aalto University, Espoo, Finland

ABSTRACT

We have studied experimentally the effect of different initial iron contamination levels on the electrical device properties of p-type Czochralski-silicon solar cells. By systematically varying phosphorus diffusion gettering (PDG) parameters, we demonstrate a strong correlation between the open-circuit voltage (V_{oc}) and the gettering efficiency. Similar correlation is also obtained for the short-circuit current (J_{sc}), but phosphorus dependency somewhat complicates the interpretation: the higher the phosphorus content not only the better the gettering efficiency but also the stronger the emitter recombination. With initial bulk iron concentration as high as $2 \times 10^{14}\,\mathrm{cm}^{-3}$, conversion efficiencies comparable with non-contaminated cells were obtained, which demonstrates the enormous potential of PDG. The results also clearly reveal the importance of well-designed PDG: to achieve best results, the gettering parameters used for high purity silicon should be chosen differently as compared with for a material with high impurity content. Finally we discuss the possibility of achieving efficient gettering without deteriorating the emitter performance by combining a selective emitter with a PDG treatment. Copyright © 2012 John Wiley & Sons, Ltd.

KEYWORDS

monocrystalline silicon; iron; phosphorus diffusion gettering; silicon solar cells

***Correspondence**

Ville Vähänissi, Department of Micro and Nanosciences, Aalto University, Espoo, Finland.
E-mail: ville.vahanissi@aalto.fi

Received 2 September 2011; Revised 24 February 2012; Accepted 15 March 2012

1. INTRODUCTION

Iron impurities are well known to degrade the solar cell performance [1]. Pioneering research to address the effects of iron on the final cell properties has been carried out already in 1980 by Davis *et al*. [2]. Because of the numerous improvements in cell processing, increased use of cheaper starting material with lesser purity and increased knowledge about the properties of iron in silicon, the topic has been addressed over and over.

Firstly, there are quite many recent studies on final cell tolerance to impurities. Dubois *et al*. [3] and Laades *et al*. [4] have experimentally shown that in an industrial single crystalline silicon solar cell process ($\eta \approx 14$–17%), silicon with moderate initial interstitial iron concentration (below $2 \times 10^{12}\,\mathrm{cm}^{-3}$) can be used without affecting the final conversion efficiency. Of course in cells targeting higher efficiency, the tolerable iron concentration is likely to be lower. Similar research has also been performed for multicrystalline silicon (mc-Si) ($\eta \approx 14$–16%). Coletti *et al*. [5] and Dubois *et al*. [6] have experimentally shown that an initial iron concentration at or below $1 \times 10^{13}\,\mathrm{cm}^{-3}$ has no observable influence on the conversion efficiency in industrially processed mc-Si solar cells.

Secondly, to address the question on how the harmful effect of increased iron contamination could be minimized in cell processing, many research efforts have been put on gettering. Phosphorus diffusion gettering (PDG) is a well-known method to relocate iron from the bulk to the emitter, where it is less harmful and thus prevents the degradation. One major advantage of PDG is that it occurs naturally in the solar cell process. There are several studies on this topic too, both experimental and theoretical ones [7–13].

Even though both the gettering and the tolerance of iron for solar cell operation have received a considerable amount of attention, there is a need for systematic studies that would concentrate on both issues simultaneously. This is actually quite relevant because these issues are often related to each other. As mentioned, the studies on the effect of increased iron impurity of the starting material on the final cell properties are often concentrated on the maximum tolerated concentration in an industrial cell process with little emphasis on PDG parameters [3–6]. On the other hand in gettering studies, the efficiency of

PDG is often evaluated on the basis of the measured recombination lifetime or the remaining bulk iron concentration, but no clear information is available how it affects the actual cell parameters [9–11,13,14]. The best lifetime does not automatically lead to the best conversion efficiency, because at some point iron gettered to the emitter might start to increase emitter recombination. In addition the maximized phosphorus content that increases the gettering efficiency can deteriorate the cell performance. In this paper, we study how the impurity tolerance can be affected by changing the phosphorus gettering parameters. The impact is evaluated by measuring the final solar cell parameters as a function of iron level in the bulk. The gettering mechanism is also examined in more detail. Finally the possibility of tailoring the PDG parameters to the specific starting material and combining a selective emitter with a PDG treatment is discussed.

2. EXPERIMENTAL

Silicon wafers with three different initial iron contamination levels, (i) $1 \times 10^{13}\,\mathrm{cm}^{-3}$ (medium), (ii) $2 \times 10^{14}\,\mathrm{cm}^{-3}$ (high) and (iii) no intentional iron, were used to fabricate solar cells. The experimental cell size was $2 \times 2\,\mathrm{cm}^2$, and on each wafer, there were seven isolated cells. Together with the cells, reference wafers, without cell structures but with identical contamination and heat treatments, were processed. The wafers used in the experiments were boron-doped p-type, <100>-oriented IC-grade magnetic Czochralski-grown wafers with a diameter of 100 mm. The thickness of the wafers was 400 μm, the resistivity was 2.7–3.0 Ω cm and the wafers had a low initial oxygen level (7–9 ppma).

As a first process step, most of the wafers were intentionally iron contaminated by immersing them in an iron-spiked $NH_4OH:H_2O_2:H_2O$ solution. Iron was diffused into the wafers with a subsequent heat treatment, the temperature of which determined the resulting contamination level. Here two different heat treatments resulting in two different iron levels were used. The iron in-diffusion heat treatments were 940 °C for 50 min and 850 °C for 55 min, resulting in bulk iron concentrations of 2×10^{14} and $1 \times 10^{13}\,\mathrm{cm}^{-3}$, respectively. The values were measured from reference wafers using the surface photovoltage (SPV) method. After iron in-diffusion, the surface contamination was removed from the wafers by etching in a $H_2O:HF:H_2O_2$ (24 : 1 : 1) solution and by RCA cleaning.

The actual solar cell process began by growing a dry oxide of about 98-nm thickness on the wafers through a 160-min oxidation at 1000 °C. The oxide on the backside of the wafers was then protected and the front side oxide was patterned with lithography and BHF etching to form openings for the emitter diffusion. The next step was emitter formation by application of phosphorus spin-on dopant (Filmtronics P509, Butler, PA, USA) and a subsequent phosphorus diffusion gettering heat treatment. Five different PDG treatments were used, each consisting of a 30-min or 60-min diffusion step at 870 °C followed by unloading or an optional lower temperature tail. Afterwards, the wafers were divided into five groups based on the applied PDG treatment. Each group contained one wafer with no intentional iron contamination, one wafer with $1 \times 10^{13}\,\mathrm{cm}^{-3}$ iron level and two wafers with $2 \times 10^{14}\,\mathrm{cm}^{-3}$ iron level. After the PDG treatment, the remaining spin-on glass and the backside oxide were etched away in $H_2O:HF$ (10 : 1), the wafers were SC-1 cleaned and the resulting emitter sheet resistances were measured with four-point probe. Five different PDG treatments used in the experiments and the resulting sheet resistances are presented in Table I.

Iron concentrations in the wafer bulk were measured from the reference wafers using the SPV method, which is a well-known method to measure interstitial iron at low concentrations. Because all iron is expected to be in the interstitial form in the bulk (also confirmed later by additional experiments), SPV measurements give us the total bulk iron concentration. The measurement procedure is as follows: first, the minority carrier diffusion lengths ($L_{n,FeB}$) are measured when iron is paired with boron (Fe_iB_s). Then the pairs are dissociated by illumination and the diffusion lengths ($L_{n,Fei}$) are re-measured now under the recombination properties determined by interstitial iron (Fe_i). Finally the interstitial iron concentration in the wafer bulk can be calculated according to the equation [15]

$$[\mathrm{Fe_i}] = 7.8 \times 10^{15} \times \left(\frac{1}{L^2_{\mathrm{n,Fe_i}}} - \frac{1}{L^2_{\mathrm{n,Fe_iB_s}}} \right) \quad [\mathrm{cm}^{-3}], \quad (1)$$

where the diffusion length values have to be inserted in micrometers. The prefactor was determined by combined deep level transient spectroscopy and SPV measurements on several samples with different iron concentrations. In addition, iron concentration in the phosphorus-doped layer was measured by secondary ion mass spectrometry (SIMS) in selected samples. SIMS measures directly the total iron concentration, which makes it a suitable method for emitter profiling.

After emitter formation, the solar cell process continued with the deposition of a SiN_x antireflection coating (ARC) by plasma-enhanced chemical vapor deposition. The thickness of the ARC was measured by ellipsometer to be 73 ± 3 nm and the refractive index 1.98 ± 0.01. The ARC deposition was followed by backside metallization. An aluminum layer with a thickness of 500 nm was sputtered

Table I. The PDG treatments used in the experiments and the resulting sheet resistances.

Group	Temperature profile	Sheet resistance [Ω/□]
30A	30 min at 870 °C + pullout at 870 °C	36
30B	30 min at 870 °C + pullout at 800 °C	35
60A	60 min at 870 °C + pullout at 870 °C	27
60B	60 min at 870 °C + pullout at 800 °C	26
60C	60 min at 870 °C + 2 h at 800 °C	24

on the backside of the wafers followed by aluminum sintering at 450 °C for 30 min.

Front side metallization with a finger width of 10 µm and a spacing of 1 mm was the last processing step. First, the ARC was patterned with lithography and reactive ion etching. Then a 50-nm-thick Ti/W layer and a 150-nm-thick Cu layer were sputtered on the wafers. The metal layers were patterned by lift-off, and finally, the cells were finished by increasing the thickness of the copper fingers via electroplating to a thickness of 7 µm. The cross-section of a finished cell is presented in Figure 1.

The electrical device properties of the finished cells were measured under the standard illumination condition (AM1.5 G, 1000 W m^{-2}, 25 °C) with the irradiance decay cell analysis method [16]. The cells were also characterized by external quantum efficiency (EQE) measurements.

Finally, the following supplementary experiments were performed in order to more accurately determine the location of the gettered iron and to demonstrate that the interstitial iron concentration in the bulk measured by SPV equals the total bulk iron concentration. Samples for these experiments were chosen from the reference wafers of the 60C group (Table I). These wafers were divided into three batches: (i) the emitter surface was etched to the depth of approximately 1 µm, (ii) both surfaces (emitter and back surface) were etched away and (iii) the wafers were left as they were. Then all batches were annealed at 1000 °C, higher than the applied iron in-diffusion temperature, for 20 min followed by fast cooling. The purpose of the anneal was to return the iron to the interstitial form in the bulk. After the anneal, the interstitial bulk iron concentration was measured by SPV.

3. RESULTS

3.1. Iron and phosphorus profiles

Figure 2 shows a summary of the measured iron concentration in the bulk after different PDG treatments. Several interesting observations can be made. Firstly, as expected, in all samples the bulk iron concentration has decreased significantly from the initial value, even in the case of light P diffusion and fast cooling (30A), in which the decrease is one decade. PDG is naturally improved with increasing P concentration and with a low temperature tail. Secondly, if we compare the initial contamination levels, the duration of the phosphorus diffusion step in the PDG treatment (30 vs 60 min) seems to be more critical for the final gettering efficiency in samples with high initial iron contamination.

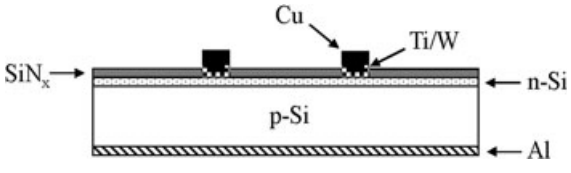

Figure 1. The solar cell structure used in the experiments.

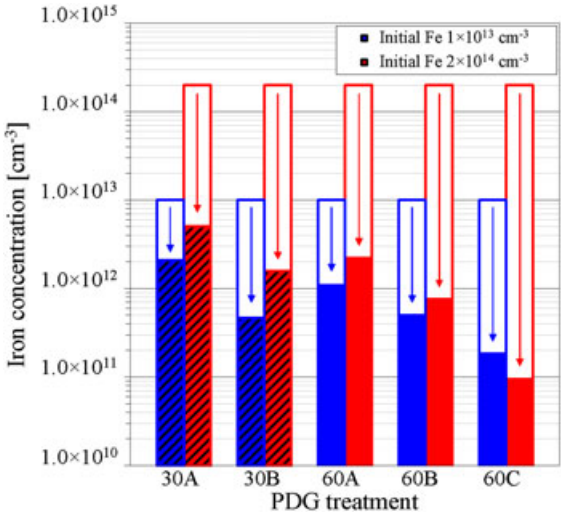

Figure 2. Measured interstitial iron concentration in the bulk after various phosphorus diffusion gettering treatments. Striped columns represent cells with 30-min P diffusion and single-colored columns cells with 60-min P diffusion. The error estimate of the interstitial iron concentration value is ±2% when iron concentration is below 1×10^{12} cm^{-3} and ±4% when iron concentration is above 1×10^{12} cm^{-3}.

The most interesting result is, however, obtained with the 60C treatment: it is clearly the most efficient one, but most importantly, the remaining iron concentrations in the bulk are opposite to the starting contamination levels. In other words, the iron concentration in the bulk of the initially highly contaminated sample after the 60C treatment is lower than in the sample with medium initial iron level and vice versa. This result is later discussed both from the gettering and cell result point-of-view.

Phosphorus and iron profiles near the wafer surface measured by SIMS from the high-contaminated and medium-contaminated wafers after PDG treatments 30B and 60B are depicted in Figure 3. These treatments were chosen as we wanted to study the influence of different phosphorus profiles in otherwise identical wafers. The obtained phosphorus profiles follow the so-called kink and tail profile typical for diffusion of high concentration of phosphorus in silicon. The peak P concentration after both PDG treatments is approximately 1×10^{21} cm^{-3} exceeding the solid solubility [17] value at 870 °C. However, the thickness of the highly doped area ($>10^{20}$ cm^{-3}) is almost doubled as a result of the increased phosphorus diffusion time. The longer P diffusion time also increases the junction depth from 0.55 to 0.75 µm.

According to Figure 2, the gettered amount of bulk iron after each PDG treatment is considerably higher in highly contaminated samples. For example, after the 60B treatment, the difference in the amount of gettered iron between highly and medium-contaminated samples is approximately 6×10^{14} atoms. If all this iron is present at the emitter, it should be clearly visible in the SIMS profiles.

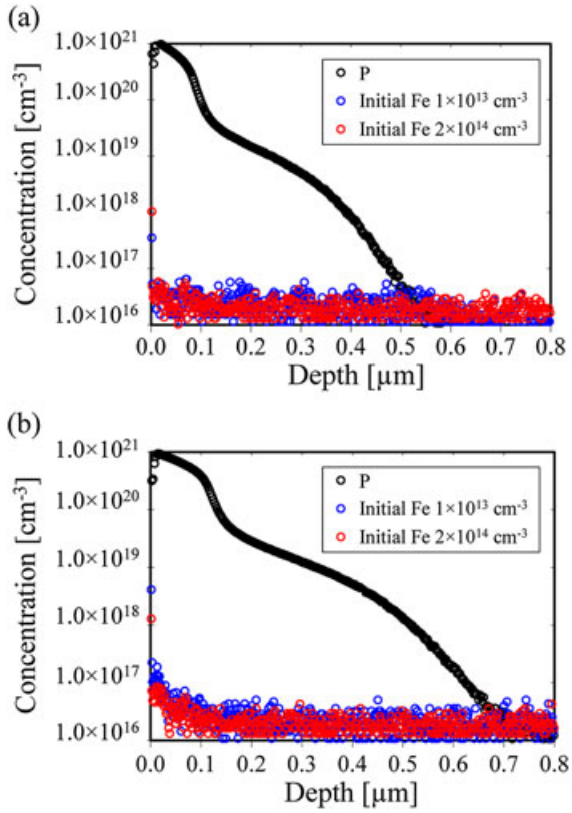

Figure 3. Phosphorus and iron profiles near the wafer surface measured by secondary ion mass spectrometry from the high-contaminated and medium-contaminated reference wafers after phosphorus diffusion gettering treatments (a) 30B and (b) 60B.

However, the measurements show that almost the same amount of iron is gettered at the emitter regardless of the initial iron level. In medium-contaminated samples, the iron profiles correspond to the amount of gettered bulk iron, but in highly contaminated samples, the location of the gettered extra iron remains unclear. In any case, the iron profiles do show that with both initial contamination levels, iron is collected to a thin surface layer, much thinner than the P-doped layer.

The SIMS results motivated us to conduct the supplementary experiments to reveal the location of the gettered extra iron present in highly contaminated samples. In the experiments, either the emitter or both surfaces were removed, which was followed by high temperature anneal. The obtained interstitial iron concentrations for the initially high and medium iron-contaminated samples of batch one (emitter removed) were 3.0×10^{11} and $1.9 \times 10^{11}\,\mathrm{cm}^{-3}$ and for batch two (both surfaces removed) 2.6×10^{11} and $2.0 \times 10^{11}\,\mathrm{cm}^{-3}$, respectively. Because we detected no significant increase in the values compared with Figure 2, we can conclude that the interstitial iron concentration in the bulk measured by SPV is truly the total bulk iron concentration. For batch three (bare high temperature anneal after spin-on glass removal) the obtained concentrations were 2.2×10^{12} and $4.3 \times 10^{12}\,\mathrm{cm}^{-3}$ for the initially high and medium iron-contaminated samples, respectively. Intriguingly the inversion of the final bulk iron concentrations in the 60C-treated samples, seen already in Figure 2, remained also after this high temperature anneal. These results are later discussed further.

3.2. Device properties of the cells

Figure 4 presents the measured electrical device properties: (a) open-circuit voltage V_{oc}, (b) short-circuit current density J_{sc} and (c) conversion efficiency η of the final solar cells after different PDG treatments. The device properties are presented both as a function of the PDG treatment and the final bulk iron concentration. The cells were measured under the standard illumination condition (AM1.5 G, 1000 W m^{-2}, 25 °C).

The measured V_{oc} values seem to be directly affected by the final iron level in the bulk leading to a strong correlation between V_{oc} and iron concentration. We clearly notice a substantial increase in V_{oc} with diminishing bulk iron concentration. Even the inversion of the bulk iron concentrations in the 60C-treated cells is visible in the open-circuit voltages. By comparing the non-contaminated cells, it is clear that the obtainable V_{oc} is nearly independent on the used PDG treatment. Notice that with the most efficient gettering treatment used here, 60C, we were able to recover the V_{oc} of the highly contaminated cells, with an increase of up to 20 mV, back to the same level as the open-circuit voltages of the non-contaminated cells.

The obtained short-circuit current density values (J_{sc}) are also interesting (Figure 4(b)). We obtain a correlation between the J_{sc} and the iron concentration, but J_{sc} is also clearly dependent on the used PDG treatment. This can be seen by comparing the non-contaminated cells, where the J_{sc} values decrease with increasing PDG duration. Thus, we obtain an individual correlation between the J_{sc} and the final iron concentration for each PDG treatment. With the highly contaminated cells, we obtain a significant improvement in the J_{sc} value only with the most efficient PDG treatment (60C). With this treatment, J_{sc} is equal compared with a non-contaminated cell. However, this value is notably lower than the best one, which is obtained from the non-contaminated cells with the 30A treatment.

The fill factor (*FF*) values of the cells vary between 0.760 and 0.780 and no trends with PDG treatments are observed. There is neither a correlation between the *FF* and the bulk iron concentration nor between the *FF* and the applied PDG treatment. This is contrary to the results reported by Macdonald *et al.* [18]. They showed that even with low contamination levels, the interstitial iron in the bulk reduces fill factors significantly. However, in their study, the reduced fill factors were in the vicinity of 0.790. Because the fill factors achieved here are around 0.775, we can state that our *FF*s are limited by some other factor than the interstitial iron.

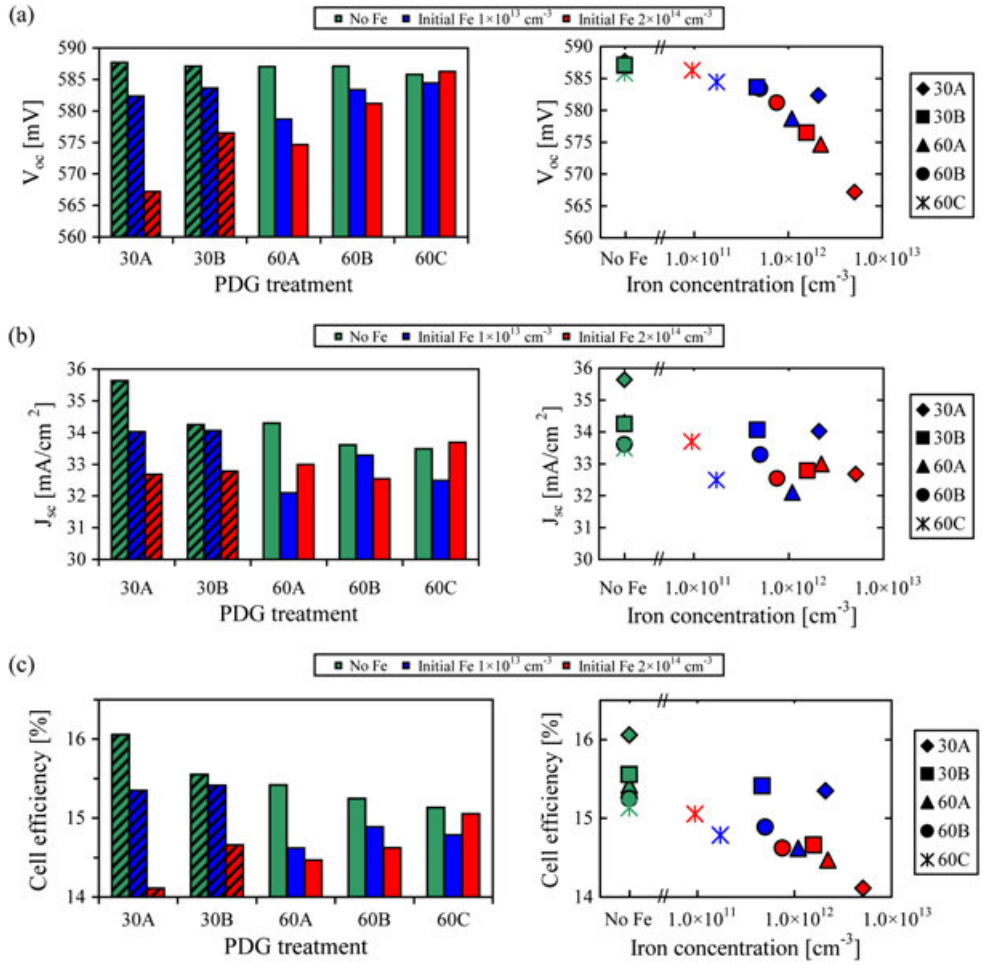

Figure 4. The measured electrical device properties: (a) open-circuit voltage V_{oc}, (b) short-circuit current density J_{sc} and (c) conversion efficiency η of the solar cells measured under the standard illumination condition (AM1.5 G, 1000 W m^{-2}, 25 °C).

The behavior of the conversion efficiency of the cells with different bulk iron concentrations and PDG treatments is a result of the combined effects of the V_{oc}, J_{sc} and *FF* described previously. As can be seen from Figure 4(c), the efficiency values are indeed in correlation with the bulk iron concentration and the applied PDG treatment. Similarly as in the case of V_{oc}, the efficiency of the highly contaminated cells significantly improves as the bulk iron concentration decreases. However, there is a significant decrease in the conversion efficiency of the non-contaminated cells with longer PDG treatments, which is dominated by the J_{sc} behavior. With medium contamination level, the improvement in V_{oc} is balanced by a decrease in J_{sc} between PDG treatments 30A and 30B, but with longer P diffusion, the cell efficiency is reduced because of the decrease in J_{sc}.

Before the cell measurements, the bulk iron was left to pair up with boron forming Fe_iB_s pairs. The pairs were not split up before the measurements and thus they determined the recombination properties. According to Schmidt [19], the dissociation of Fe_iB_s pairs leads to degradation in most cell parameters, including V_{oc}, J_{sc}, *FF* and η. Had the Fe_iB_s pairs been dissociated before the measurements by, for example, illumination, the observed degradation of the cell parameters as a function of final bulk iron concentration would have been even stronger.

3.3. EQE of the cells

Figure 5 shows the influence of the PDG treatments and iron levels on the EQE of the selected cells. The EQE results are comparable with each other, because the optical properties of the ARCs were measured to be identical from cell to cell. In addition, the light transmission through the device can be neglected due to the thickness (400 μm) and the used cell structure.

A rather poor performance with short wavelengths is seen in all cells in Figure 5. The P concentration of the spin-on dopant used for the diffusion was 2.0×10^{21} cm^{-3}. This rather high concentration naturally leads to high P concentration and consequently to strong Auger

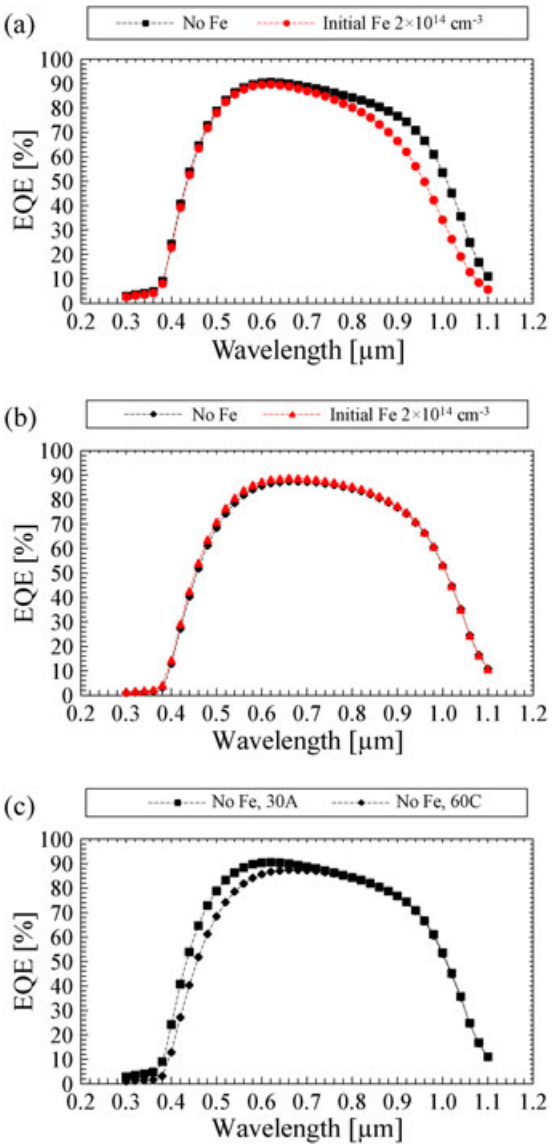

Figure 5. The influence of different phosphorus diffusion gettering treatments and iron levels on the external quantum efficiency of the cells. Results are shown for (a) 30A-treated non-contaminated and highly contaminated cells, (b) 60C-treated non-contaminated and highly contaminated cells and (c) 30A-treated and 60C-treated non-contaminated cells.

recombination in the junction area after in-diffusion. The charge carrier concentration at the emitter is close to the solid solubility of P at the applied diffusion temperature. On the other hand, P concentration near the emitter surface exceeds the solid solubility value, which leads to the formation of electrically inactive P. This, in turn results in a so-called dead layer with extremely high recombination rate near the cell surface. With emitter P concentration above $10^{20}\,\mathrm{cm}^{-3}$, the Auger recombination-limited lifetime drops below 1 ns [20], which corresponds to a diffusion length of about 300 nm. Figure 3 shows that P concentration at the emitter surface is well above $10^{20}\,\mathrm{cm}^{-3}$ already after the 30B treatment (similar in-diffusion step as in 30A). The resulting minority carrier diffusion length in the range of 300 nm is evidently too short for collecting holes generated near the emitter surface. In summary, the dead layer together with the significant Auger recombination explains the poor cell performance with short wavelengths.

Nonetheless, we can make several observations from the EQE results. In Figure 5(a), EQE of non-contaminated and highly contaminated cells are compared after PDG treatment 30A. At short wavelengths, the obtained EQE curves overlap totally, as the light is absorbed in the emitter region, consequently describing the recombination behavior of carriers there. However, only negligible absorption occurs in the emitter region because the absorption depth of light with wavelengths above 700 nm is longer than 5.3 µm. According to Figure 4(c), there was a clear difference in the conversion efficiency. This is confirmed by the EQE deviation at longer wavelengths, that is, due to the increased amount of iron in the bulk.

In Figure 5(b), the EQE of the non-contaminated and highly contaminated cells that have gone through the most efficient PDG treatment used here, 60C, are compared. Intriguingly the obtained curves overlap at all wavelengths, and there is no deviation even at long wavelengths indicating that the final cell performance of the initially highly contaminated cell is not limited by the iron contamination. This confirms the previous almost identical *I–V* results and proves that the used gettering treatment truly erases the negative effect of the initially high iron concentration.

The EQE of 30A-treated and 60C-treated non-contaminated cells are compared in Figure 5(c). The obtained curves overlap at wavelengths longer than 700 nm and then start to deviate at shorter wavelengths. The overlapping at long wavelengths indicates that the bulk recombination lifetime and the back-surface recombination in the cells are identical. The difference in the final cell performances seen in Figure 4(c) is explained entirely by the deviation at shorter wavelengths and more closely by the recombination behavior in the emitter region.

The difference in the emitter recombination can be explained by the different PDG treatments applied in the fabrication process. A longer high temperature in-diffusion step and a long low temperature tail result in increased emitter P concentration and expanded emitter region (Figure 3). From the SIMS results, we can estimate the magnitude of these effects on the final cell. As stated earlier, the minority carrier diffusion length in the dead layer drops below 300 nm meaning that no carriers generated there will be collected. Therefore, if the dead layer thickness increases from 0.1 to 0.2 µm, the light absorbed within the first 0.2 µm cannot be utilized. Under the AM1.5 G spectrum, the dead layer thickening can be calculated to cause approximately a 5% decrease in J_{sc}, which roughly explains the observed difference between 30A-treated and 60C-treated non-contaminated cells.

4. DISCUSSION

The iron concentration in the bulk after each PDG treatment in the medium contamination level samples (Figure 2) behaves as expected from previous publications [8–10]. However, in the highly contaminated samples, "too efficient" gettering and the inversion of the remaining bulk iron concentrations after the 60C treatment are in contradiction with the results presented in [8]. In that study, the ratio between bulk iron concentrations in initially highly versus medium-contaminated samples remained constant after each PDG treatment. Our results suggest that there is another gettering mechanism present in the experiments in addition to the assumed conventional segregation. For the second mechanism, there are several options: iron might have (i) gettered by phosphorus clusters or phosphorus precipitates in the emitter, (ii) gettered internally (bulk precipitation), (iii) precipitated at the back surface or (iv) gettered to the phosphorus glass or glass–silicon interface. The SIMS and surface etching results rule out all the other options except the last one. Thus it seems that during the process, some iron is lost from the wafer and this effect is stronger in the initially highly contaminated samples.

Our hypothesis is that the spin-on glass/silicon interface layer acts as a sink for the iron that is segregated to the emitter. The difference in bulk iron concentration after gettering between high and medium iron samples decreases as the gettering time increases and finally the remaining iron levels even invert with the 60C treatment. This indicates that the extra gettering mechanism is active during the whole PDG treatment. The fact that the effect is stronger in the highly contaminated case suggests that it involves iron precipitation as higher iron contamination causes a faster precipitation rate. As the bulk iron concentration is undersaturated, segregation driven only by the solubility difference under equilibrium cannot lead to iron precipitation. However, iron precipitation could be enabled by non-equilibrium conditions. It has been proposed that metal precipitation in the emitter is caused by local supersaturation of self-interstitials, for example, by growing SiP precipitates [21]. The local supersaturation of self-interstitials can cause precipitation of metals such as nickel and iron as growth of their silicides is associated to a volume shrinkage. The local supersaturation of self-interstitials can induce a flux of substitutional metals toward the self-interstitial sinks and cause the precipitation of metals at the sink when the concentration exceeds the thermal equilibrium value [22–24]. However, it is also claimed that in the latter process only the supersaturation of self-interstitials should be critical [24], although according to our observation also the iron concentration strongly affects the precipitation rate. The extra gettered iron is not visible in the SIMS measurements, as the glass and very thin surface layer, where the iron is most likely gettered, is almost completely etched away during the removal of the spin-on glass and the following SC-1 cleaning. This might support the idea that SiP precipitates have an important effect on iron precipitation but not on segregation as SiP precipitates are source for phosphorus and located close to the glass silicon interface [25].

As mentioned in the introduction, we thought that the cell efficiency would start to decrease due to the increased emitter recombination influenced by the iron impurities gettered there. However, this was not the case even in the highly contaminated samples. This agrees with the results reported by Macdonald *et al*. [26]. According to their studies, P-diffused emitters are immune to the presence of high levels of iron ($10^{16}\,cm^{-3}$). In our samples, in addition to segregation to the emitter, iron ended up also in the phosphorus glass. As a result, the maximum getterable amount of bulk iron through phosphorus diffusion significantly increases further without influencing the emitter negatively.

Even though emitter recombination due to gettered iron does not seem to be a problem, there is inevitably a compromise between cell efficiency and the gettering efficiency. If rather clean cells go through a gettering step designed for highly contaminated cells and vice versa, the resulting efficiencies will not be as high as could be achievable. Notice that we achieved no improvement in cell efficiency by increasing the gettering efficiency with medium contamination level cells. The weight of the emitter P profile in comparison with gettering efficiency seems to increase with the decreasing contamination level. The optimum treatment for different silicon material (e.g., upgraded metallurgical-grade Si and solar-grade Si) therefore varies a lot. One possibility is to split the wafers into different batches based on their initial iron concentration. Each batch should be then treated with different P in-diffusion and gettering steps for maximum performance. Because the contamination level in a silicon ingot usually changes with position, the splitting could be easily performed based on the ingot position.

A recent trend of adding the selective emitter capability in high-efficiency crystalline silicon solar cell turnkey lines [27] could remove the need for the aforementioned compromise between P profile and gettering efficiency. In selective emitters, only the areas under the contacts are heavily doped, approximately to the same P level as used here, ensuring a low contact resistance. Elsewhere the doping level is much lower, optimizing the emitter saturation current and diffusion length. The selective emitter enables the exploitation of more effective PDG treatments at lower temperatures without deteriorating the emitter performance. This could compensate the loss in gettering efficiency at high temperatures. However, in selective emitters, the finger separation could limit the total obtainable gettering efficiency to some extent: with short gettering treatments, not necessarily all the metals have enough time to diffuse to the gettering site. This fact should be taken into account when designing the optimal PDG treatment. All in all the combination of a selective emitter and a well-designed PDG treatment could be very beneficial to the final cell performance.

5. CONCLUSIONS

We have carried out a systematic study of the effect of different initial iron contamination levels on the electrical device properties of single crystalline silicon solar cells. A special emphasis was put on varying PDG treatments. By using a special PDG treatment, we were able to restore the conversion efficiency of highly iron-contaminated cells (2×10^{14} cm^{-3}) to a level comparable with the non-contaminated cells. We also demonstrated that even high amounts of gettered bulk iron do not increase the emitter recombination because, quite surprisingly, all iron is not necessarily gettered at the emitter. This clearly shows that with suitable PDG, it is possible to increase the maximum tolerable impurity concentration and prevent the otherwise obvious degradation of the cell performance.

In addition, our results clearly show that the most efficient gettering treatment is not always the best option for the solar cell operation. A PDG treatment, which was not optimized for the initial contamination level of the cell, was seen to negatively affect the emitter quality and thus the performance of the cell was deteriorated. We discussed the possibility of using a slightly varying PDG treatment depending on the contamination level of the starting wafers. All in all our results demonstrate the enormous potential of PDG but also emphasize the importance of designing both P in-diffusion and gettering steps together well for the optimum net effect.

ACKNOWLEDGEMENTS

The authors acknowledge the financial support from the Finnish National Technology Agency, Academy of Finland, Okmetic Oyj, Endeas Oy, Semilab Inc. and VTI Technologies Oy. The corresponding author thanks Jenny and Antti Wihuri Foundation and the Graduate School in Electronics, Telecommunications and Automation (GETA) for financial support. In addition, the processing assistance provided by the students of the Semiconductor Technology Laboratory Course at Aalto University is appreciated.

REFERENCES

1. Istratov AA, Hieslmair H, Weber ER. Iron contamination in silicon technology. *Applied Physics A: Materials Science and Processing* 2000; **70**: 489–534. DOI: 10.1007/s003390000458
2. Davis JR, Rohatgi A, Hopkins RH, Blais PD, Rai-Choudhury P, McCormick JR, Mollenkopf HC. Impurities in silicon solar cells. *IEEE Transactions on Electron Devices* 1980; **27**: 677–687.
3. Dubois S, Palais O, Pasquinelli M, Martinuzzi S, Jaussaud C, Rondel N. Influence of iron contamination on the performances of single-crystalline silicon solar cells: computed and experimental results. *Journal of Applied Physics* 2006; **100**: 024510. DOI: 10.1063/1.2218593
4. Laades A, Lauer K, Bähr M, Maier C, Lawerenz A, Alber D, Nutsch J, Lossen J, Koitzsch C, Kibizov R. Impact of iron contamination on CZ-silicon solar cells. *Proceedings of the 24th European Photovoltaic Solar Energy Conference and Exhibition*, Hamburg, Germany, 2009; 1728–1732.
5. Coletti G, Bronsveld PC, Hahn G, Warta W, Macdonald D, Ceccaroli B, Wambach K, Le Quang N, Fernandez JM. Impact of metal contamination in silicon solar cells. *Advanced Functional Materials* 2011; **21**: 879–890. DOI: 10.1002/adfm.201000849
6. Dubois S, Palais O, Ribeyron PJ, Enjalbert N, Pasquinelli M, Martinuzzi S. Effect of intentional bulk contamination with iron on multicrystalline silicon solar cell properties. *Journal of Applied Physics* 2007; **102**: 083525. DOI: 10.1063/1.2799057
7. Nadahara S, Tsunoda H, Shiozaki M, Watanabe M, Yamabe K. Low temperature phosphorus diffusion gettering of iron in silicon. In Defects in Silicon II, Proceedings of the Second Symposium on Defects in Silicon, Bullis WM, Gösele U, Shimura F (eds). Electrochemical Society: Pennington, NJ, 1991; 667–674.
8. Shabani MB, Yamashita T, Morita E. Study of gettering mechanisms in silicon: competitive gettering between phosphorus diffusion gettering and other gettering sites. *Solid State Phenomena* 2008; **131–133**: 399–404. DOI: 10.4028/www.scientific.net/SSP.131-133.399
9. Phang SP, Macdonald D. Direct comparison of boron, phosphorus, and aluminum gettering of iron in crystalline silicon. *Journal of Applied Physics* 2011; **109**: 073521. DOI: 10.1063/1.3569890
10. Talvitie H, Vähänissi V, Haarahiltunen A, Yli-Koski M, Savin H. Phosphorus and boron diffusion gettering of iron in monocrystalline silicon. *Journal of Applied Physics* 2011; **109**: 093505. DOI: 10.1063/1.3582086
11. Bentzen A, Holt A, Kopecek R, Stokkan G, Christensen JS, Svensson BG. Gettering of transition metal impurities during phosphorus emitter diffusion in multicrystalline silicon solar cell processing. *Journal of Applied Physics* 2006; **99**: 093509. DOI: 10.1063/1.2194387
12. Haarahiltunen A, Savin H, Yli-Koski M, Talvitie H, Sinkkonen J. Modeling phosphorus diffusion gettering of iron in single crystal silicon. *Journal of Applied Physics* 2009; **105**: 023510. DOI: 10.1063/1.3068337
13. Hofstetter J, Lelièvre JF, Fenning DP, Bertoni MI, Buonassisi T, Luque A, del Cañizo C. Enhanced iron gettering by short, optimized low-temperature annealing after phosphorus emitter diffusion for industrial silicon solar cell processing. *Physica Status Solidi C* 2011; **8**: 759–762. DOI: 10.1002/pssc.201000334
14. Härkönen J, Lempinen VP, Juvonen T, Kylmäluoma J. Recovery of minority carrier lifetime in low-cost multicrystalline silicon. *Solar Energy Materials & Solar*

Cells 2002; **73**: 125–130. DOI: 10.1016/S0927-0248(01)00117-9

15. Yli-Koski M, Palokangas M, Sokolov V, Storgårds J, Väinölä H, Holmberg H, Sinkkonen J. Recombination activity of iron in boron doped silicon. *Physica Scripta* 2002; **T101**: 86–88. DOI: 10.1238/Physica.Topical.101a00086
16. Hyvärinen J, Karila J. New analysis method for crystalline silicon cells. *Proceedings of the 3rd World Conference on Photovoltaic Energy Conversion*, Osaka, Japan, 2003; 1521–1524.
17. Borisenko VE, Yudin SG. Steady-state solubility of substitutional impurities in silicon. *Physica Status Solidi A* 1987; **101**: 123–127. DOI:10.1002/pssa.2211010113
18. Macdonald D, Cuevas A. Reduced fill factors in multicrystalline silicon solar cells due to injection-level dependent bulk recombination lifetimes. *Progress in Photovoltaics: Research and Applications* 2000; **8**: 363–375. DOI: 10.1002/1099-159X(200007/08)8:4<363::AID-PIP328>3.0.CO;2-Y
19. Schmidt J. Effect of dissociation of iron-boron pairs in crystalline silicon on solar cell properties. *Progress in Photovoltaics: Research and Applications* 2005; **13**: 325–331. DOI: 10.1002/pip.594
20. Kerr MJ, Cuevas A. General parameterization of Auger recombination in crystalline silicon. *Journal of Applied Physics* 2002; **91**: 2473–2480. DOI: 10.1063/1.1432476
21. Ourmazd A, Schröter W. Phosphorus gettering and intrinsic gettering of nickel in silicon. *Applied Physics Letters* 1984; **45**: 781–783. DOI: 10.1063/1.95364
22. Schröter W, Kuhnapfel R. Model describing phosphorus diffusion gettering of transition elements in silicon. *Applied Physics Letters* 1990; **56**: 2207–2209. DOI: 10.1063/1.102968
23. Spiecker E, Seibt M, Schröter W. Phosphorus-diffusion gettering in the presence of a nonequilibrium concentration of silicon interstitials: a quantitative model. *Physical Review B* 1997; **55**: 9577–9583. DOI: 10.1103/PhysRevB.55.9577
24. Schröter W, Seibt M, Gilles D. High-temperature properties of 3d transition elements in silicon. In Materials Science and Technology, **4**, Chan RW, Haasen P, Kramer EJ, Schröter W (eds). VCH: Weinheim, 1991; 539–589.
25. Vais V, Mrcarica M, Braña AF, Leo T, Fernandez JM. Mechanisms involved in the formation of phosphosilicate glass from a phosphoric acid dopant source. *Progress in Photovoltaics: Research and Applications* 2011; **19**: 280–285. DOI: 10.1002/pip.1023
26. Macdonald D, Häckel M, Cuevas A. Effect of gettered iron on recombination in diffused regions of crystalline silicon wafers. *Applied Physics Letters* 2006; **88**: 092105. DOI: 10.1063/1.2181199
27. Chunduri SK. Be selective!. *Photon International* 2009; **11**: 108–116.